Results in Applied Mathematics 20 (2023) 100402

Contents lists available at ScienceDirect

Results in Applied Mathematics

journal homepage: www.elsevier.com/locate/results-in-applied-mathematics

Replacing voids and localized parameter changes with fictitious forcing terms in boundary-value problems

Giulio G. Giusteri [*], Fabio Marcuzzi, Laura Rinaldi

Department of Mathematics "Tullio Levi-Civita", University of Padua, via Trieste 63, Padova, 35131, Italy

ARTICLE INFO

MSC:
35R30
80A23
65M32
15A29

Keywords:
Material parameter change
Wave propagation
Diffusion
Void identification
Inverse problem

ABSTRACT

We present a general observation on how to replace changes of material properties in limited regions within a domain with fictitious forcing terms in initial- and boundary-value problems associated with wave propagation and diffusion. Then, by considering a paradigmatic heat conduction problem on a domain with a cavity, we prove that the presence of the void can be replaced by a fictitious heat source with support contained within the cavity. We illustrate this fact in a situation where the source term can be analytically recovered from the values of the temperature and heat flux at the boundary of the cavity. Our result provides a strategy to map the nonlinear geometric inverse problem of void identification into a more manageable one, that involves the identification of forcing terms given the knowledge of external boundary data. To set the stage for a systematic study of the inverse problem, we present algebraic reconstructions, based on a finite-element discretization of the domain, that give an approximation of the fictitious source from different sets of temperature measurements. We show how the accuracy of the reconstruction is reflected on the void identification.

1. Introduction

In several applications, the solution of a partial differential equation on a domain with a complex geometry can be found starting from solutions defined on a larger, but topologically simpler, domain. In particular, problems in exterior domains or domains with holes can be mapped onto problems in the whole space or in filled domains. This is for instance the case in the method of image charges for electrostatics [1] or that of singularities in low-Reynolds-number flows [2]. In those cases, the physical domain is typically known at the outset. On the other hand, in real-world applications we often deal with a limited knowledge, due to practical inaccessibility, of the physical domain over which a given process takes place and the estimation of the domain geometry is an important inverse problem.

A related question with far-reaching applications is how to identify regions within a material body where mechanical parameters, such as elastic moduli, permeability, or conductivity, differ significantly form a reference value. This could, for example, help in the recognition of pathological alterations in biological soft tissues. As a matter of fact, this can be viewed as a generalization of the void identification problem, since the absence of material is akin to an extreme change in mechanical properties.

In this work, we present a way to map the estimation of regions with altered properties into a force reconstruction problem. A specialization of such a scheme provides a way to tackle geometry estimation or void identification problems, in which the domain is unknown, as source or force identification problems stated on a fixed, known domain. To this end, we need to introduce suitable extensions of differential problems from complex domains to larger and simpler ones, in such a way that the restriction of the solution to the physical domain remains unchanged.

* Corresponding author.
E-mail address: giulio.giusteri@unipd.it (G.G. Giusteri).

https://doi.org/10.1016/j.rinam.2023.100402
Received 25 July 2023; Received in revised form 18 September 2023; Accepted 20 September 2023
Available online 3 October 2023

We will focus attention on diffusion and heat conduction problems and on linear wave propagation, that are relevant to a broad set of applications where one aims at estimating hidden material changes (such as, for instance, discontinuities of material parameters, hidden voids, material degradation, etc.) on the basis of partial measurements in prescribed regions, typically at the boundary. From the point of view of computational efficiency, this is important because the nonlinear inverse problem of geometry identification is replaced by an easier-to-solve linear inverse problem of source identification, for which numerous theoretical results and numerical approaches are available, see e.g. [3] for thermal problems.

In heat transfer there are relevant applications where void/material-change identification is the key issue. For example, in the hidden corrosion estimation problem [4], material changes occur starting from a hidden boundary and the solid material is gradually substituted with the surrounding environment (typically a fluid or a gas, like air). In the literature, there is a wide variety of mathematical techniques to solve this kind of inverse problems of detection of subsurface cavities and flaws using thermographic techniques, with a major distinction between methods based on steady-state or on transient thermal analysis. In the first group of methods, we mention the work of Kassab and Pollard [5], where it is presented a high-resolution cubic spline-based algorithm for the detection of arbitrarily shaped subsurface cavities by steady-state thermal response of the system subjected to a thermal load, also known as infrared computerized axial tomography (IR CAT), which involves the solution of an elliptic heat conduction equation and is theoretically based on the solution of the geometric inverse heat conduction problem. In the work of Divo, Kassab and Rodriguez [6], it is presented a method relying on a superposition of clusters of sources/sinks with a boundary element solution of the forward problem to solve the inverse geometric problem of detection of subsurface cavities and flaws; after locating the clusters and their strengths, a search is initiated to locate the internal geometry corresponding to the enclosed cavities that satisfies the boundary condition at the cavity side. Both the location of the clusters and associated strengths of the sources/sinks and the search for the cavity geometry are accomplished using a genetic algorithm. In the second group of methods, namely transient thermal imaging, many of the developed approaches are related to the formulation of the problem as an optimization problem, where one tries to find a minimizer of a suitable cost function, like in the book of Kirsch [7] and the work of Bryan and Caudill [8], even adopting inner-outer iterations with an adaptive parametrization, like in our previous work [9], or gradient smoothing techniques like in the work of Kazemzadeh [10]. Further, recent problems of this kind concern e.g. fractional diffusion problems, such as the one considered by Sidi et al. [11] and recent solution methods involve a scientific machine learning approach, like the one proposed by Pratama et al. [12], where it is applied to a relevant application in medical diagnosis. All these approaches formulate nonlinear inverse problems based upon temperature-prediction errors and we have already shown by mere intuition and algorithmic exploration [13] that estimating the fictitious heat source turns out to be much easier than estimating the void (or parameter change) by solving a geometric inverse problem, and much more accurate than processing the gradient of temperature-prediction errors.

In linear wave propagation problems there are also relevant applications where the problem of estimating the possibly non-homogeneous material coefficients inside a physical system, from transient excitations and measurements made in a few points on the boundary, is the key issue. For example, in non-destructive control or inspection of mechanical and civil structures and in seismic inversion, it is often formulated an inverse scattering problem [14], for which several algorithms have been proposed in the literature, e.g. travel-time and full waveform inversion (FWI) [15], layer-stripping [16], migration [17]. They follow a signal-based approach, in which the estimation of the material properties inside the system is performed by monitoring the presence and the properties of backward waves (scattered waves) produced by the presence of interfaces between different materials within the system. They are simplified formulations, somewhat empirical and alternative to the nonlinear estimation problem that a model-based approach would call for [18–20]. We will show in what follows that the nonlinear parameter estimation problem can be replaced by a linear source estimation problem, that can be solved efficiently by using, for instance, a Kalman Filter with an augmented state [21].

In linear diffusion there are also important applications where one aims at estimating the possibly non-homogeneous material coefficients from stimuli and measurements made in a few points on the boundary. For example, in Diffuse Optical Tomography (DOT) [22] the main objective is to estimate the absorption coefficient and the reduced scattering coefficient of a certain media given a set of boundary measurements. Biological tissues contain many objects, such as arteries, skin and fat, whose optical properties are rather different. When these values are close to those of the background, linear techniques are usually employed to estimate them. However, certain objects, such as tumors, may have properties which cannot be well estimated with linear models. Some authors used a nonlinear method involving an Extended Kalman Filter [23,24], because the physical parameters enter nonlinearly in the PDE, but the diffusion operator is linear and, therefore, the estimation of the tumoral region may be performed by solving a linear source estimation problem, as we will see.

We present our main idea in Section 2 with observations concerning wave propagation and diffusion problems. In Section 2.1, we prove that a heat transfer problem on a domain with an internal unknown cavity has an equivalent formulation, stated on the filled domain, in which the void presence is simulated by a fictitious source term added to the equation. This requires defining an extension of the physical solution able to ensure that proper boundary conditions at the hidden cavity surface are met. Importantly, the support of the fictitious source computed from the extension is always contained within the cavity region, thus providing a way to identify the void geometry by reconstructing that source. We exemplify the equivalence in Section 3, by working on a situation in which the fictitious source term can be analytically computed. We set the stage for further investigation of inverse problems in Section 4, wherein the reconstruction of the source from partial temperature measurements is tackled in the context of the algebraic inversion of the discretized differential problem. We show how the reconstruction is affected by the partial availability of the data and to what extent the shape of the cavity can be estimated from the approximate source term. We summarize our results and mention further research directions in Section 5.

2. The strategy

In this section, we present the scheme that allows to reformulate various homogeneous differential problems into equations featuring forcing terms able to mimic parameter changes and the presence of voids. A general and quite important result is that the fictitious forces are supported within the region of material changes or void. As we shall see, in the case of parameter changes everything stems from an extremely simple observation, while the treatment of voids requires additional care. In the latter case, the fictitious forcing terms are not unique, but we will indicate a way to make a convenient selection.

For definiteness, we will employ a common geometrical setting throughout the whole section. We consider two open and simply connected bounded domains Ω_B and Ω_C in $\mathbb{R}^n$ such that $\overline{\Omega_C} \subset \Omega_B$, where Ω_C may represent a region where mechanical parameters differ from the reference value or even a cavity within the body Ω_B. With these provisions, the domain $\Omega_D := \Omega_B \setminus \overline{\Omega_C}$ presents a single hole and we can identify the exterior and interior boundaries as $\partial\Omega_B$ and $\partial\Omega_C$, respectively, with the obvious property that $\partial\Omega_D = \partial\Omega_B \cup \partial\Omega_C$ and $\partial\Omega_B \cap \partial\Omega_C = \emptyset$. Moreover, we introduce the final time $\tau > 0$ and set differential problems on the time interval $[0, \tau]$.

We first consider the propagation of waves in the domain Ω_B. In the simplest linear and isotropic approximation, the relevant mechanical parameter in the D'Alembert equation is the wave speed c, that may be non-homogeneous. Given a reference value $c_0 > 0$, we assume

$$c(\boldsymbol{x}) = \begin{cases} c_0 & \text{if } \boldsymbol{x} \in \Omega_D, \\ c_1(\boldsymbol{x}) & \text{if } \boldsymbol{x} \in \Omega_C, \end{cases}$$

in such a way that c is a smooth function in Ω_B.

Denoting by $u : \Omega_B \times [0, \tau] \to \mathbb{R}$ any scalar field of interest, the corresponding wave equation, together with suitable initial and boundary conditions, becomes

$$\begin{cases} \partial^2_{tt} u - \operatorname{div}(c^2 \nabla u) = 0 & \text{on } \Omega_B \times [0, \tau], \\ u = g & \text{on } \partial\Omega_B \times [0, \tau], \\ u(0, \cdot) = U_0(\cdot) & \text{on } \Omega_B, \\ \partial_t u(0, \cdot) = V_0(\cdot) & \text{on } \Omega_B, \end{cases} \tag{1}$$

where g is a prescribed datum, depending on time and space, and U_0 and V_0 represent the initial conditions.

Proposition 2.1. *Given a solution $u : \Omega_B \times [0, \tau] \to \mathbb{R}$ of the differential problem (1) with smooth boundary data $g : \partial\Omega_B \times [0, \tau] \to \mathbb{R}$ and initial conditions U_0 and V_0, there exists a fictitious force field $f : \Omega_B \times [0, \tau] \to \mathbb{R}$ such that:*

(i) the function u is a solution of the differential problem

$$\begin{cases} \partial^2_{tt} u - c_0^2 \Delta u = f & \text{on } \Omega_B \times [0, \tau], \\ u = g & \text{on } \partial\Omega_B \times [0, \tau], \\ u(0, \cdot) = U_0(\cdot) & \text{on } \Omega_B, \\ \partial_t u(0, \cdot) = V_0(\cdot) & \text{on } \Omega_B, \end{cases} \tag{2}$$

(ii) $f = 0$ in the region Ω_D, where $c = c_0$.

Proof. It is immediate to verify that defining $f := \operatorname{div}[(c^2 - c_0^2)\nabla u]$ leads to (i) and (ii). □

A completely analogous statement holds for the case of diffusion equations.

Proposition 2.2. *Let $\alpha_0 > 0$ be a reference diffusivity (constant and uniform) and let $\alpha : \Omega_B \to \mathbb{R}$ be a positive and smooth function such that $\alpha = \alpha_0$ in Ω_D. Given a solution $u : \Omega_B \times [0, \tau] \to \mathbb{R}$ of the differential problem*

$$\begin{cases} \partial_t u - \operatorname{div}(\alpha \nabla u) = 0 & \text{on } \Omega_B \times [0, \tau], \\ u = g & \text{on } \partial\Omega_B \times [0, \tau], \\ u(0, \cdot) = U_0(\cdot) & \text{on } \Omega_B, \end{cases} \tag{3}$$

with smooth boundary data $g : \partial\Omega_B \times [0, \tau] \to \mathbb{R}$ and initial condition U_0, there exists a fictitious source field $f : \Omega_B \times [0, \tau] \to \mathbb{R}$ such that u is a solution of

$$\begin{cases} \partial_t u - \alpha_0 \Delta u = f & \text{on } \Omega_B \times [0, \tau], \\ u = g & \text{on } \partial\Omega_B \times [0, \tau], \\ u(0, \cdot) = U_0(\cdot) & \text{on } \Omega_B, \end{cases} \tag{4}$$

and such that $f = 0$ in Ω_D.

Proof. It is enough to define $f := \operatorname{div}[(\alpha - \alpha_0)\nabla u]$. □

As simple as they may be, the foregoing facts have important practical implications in the context of inverse problems. We can think for instance of a scenario where we wish to identify the region Ω_C in which the parameters change significantly having available only measurements of u on a portion of the boundary and a knowledge of the reference parameters. Instead of attacking the inverse problem of estimating the region itself or the values of the unknown parameters, we can find an estimate of the fictitious force f and then approximate Ω_C with the support of f. Since the force appears linearly in the equation and does not multiply any unknown, we obtain important simplifications from a computational point of view.

2.1. Heat conduction in domains with a cavity

Considering Ω_C as an actual cavity requires a more careful treatment of the equations, but we can set up a scheme parallel to what we just presented. We will illustrate this working on a heat conduction problem that, not only provides an important application for the methods we introduced, but also represents a paradigmatic case in the context of void identification procedures. In this particular setting, we show the equivalence of two differential problems in describing the evolution of the temperature field in the physical domain. Introducing the constant mass density $\rho > 0$, specific heat $c > 0$, and thermal conductivity $k > 0$, we can write the heat conduction problem for the temperature field $T : \Omega_D \times [0,\tau] \to \mathbb{R}$ as

$$\begin{cases} \rho c \partial_t T = k \Delta T & \text{on } \Omega_D \times [0,\tau], \\ k \nabla T \cdot \boldsymbol{n} = g & \text{on } \partial\Omega_B \times [0,\tau], \\ k \nabla T \cdot \boldsymbol{n} = 0 & \text{on } \partial\Omega_C \times [0,\tau], \\ T(0,\cdot) = T_0(\cdot) & \text{on } \Omega_D, \end{cases} \tag{5}$$

where $\boldsymbol{n}$ is the unit outer normal to $\partial\Omega_D$, g is a prescribed (space- and time-dependent) heat flux on the external boundary, and T_0 is the initial temperature field. For the sake of simplicity we assume a vanishing heat flux across the internal boundary $\partial\Omega_C$.

Our goal is now to prove that there exists a second differential problem, stated on the filled domain Ω_B, the solution of which is a temperature field $\tilde{T} : \Omega_B \times [0,\tau] \to \mathbb{R}$ such that $\tilde{T} = T$ on $\Omega_D \times [0,\tau]$. This problem takes the form

$$\begin{cases} \rho c \partial_t \tilde{T} = k \Delta \tilde{T} + f & \text{on } \Omega_B \times [0,\tau], \\ k \nabla \tilde{T} \cdot \boldsymbol{n} = g & \text{on } \partial\Omega_B \times [0,\tau], \\ \tilde{T}(0,\cdot) = \tilde{T}_0(\cdot) & \text{on } \Omega_B, \end{cases} \tag{6}$$

where the initial condition $\tilde{T}_0$ coincides with T_0 on Ω_D and $f : \Omega_B \times [0,\tau] \to \mathbb{R}$ is a fictitious heat source.

Theorem 2.3. *Given a solution T of the differential problem (5) with smooth boundary data g and initial condition T_0, there exists a fictitious source field f such that:*

(i) the solution $\tilde{T}$ of the differential problem (6) coincides with T on $\Omega_D \times [0,\tau]$;
(ii) $f = 0$ in the physical domain $\Omega_D \times [0,\tau]$.

Proof. Let us seek conditions on f that guarantee that $\tilde{T} = T$ on $\Omega_D \times [0,\tau]$. Denoting by ϕ a smooth test field on $\Omega_B \times [0,\tau]$, the weak formulations of problems (5) and (6) read

$$\int_{\Omega_D} \rho c \partial_t T \phi \, dx + \int_{\Omega_D} (k \nabla T) \cdot (\nabla \phi) \, dx - \int_{\partial\Omega_B} k g(x) \phi \, ds = 0, \tag{7}$$

$$\int_{\Omega_B} \rho c \partial_t \tilde{T} \phi \, dx + \int_{\Omega_B} (k \nabla \tilde{T}) \cdot (\nabla \phi) \, dx - \int_{\Omega_B} f \phi \, dx - \int_{\partial\Omega_B} k g(x) \phi \, ds = 0. \tag{8}$$

The condition $\tilde{T} = T$ on $\Omega_D \times [0,\tau]$ holds if and only if taking the difference of the two equations, we obtain

$$\int_{\Omega_C} \rho c \partial_t \tilde{T} \phi \, dx + \int_{\Omega_C} (k \nabla \tilde{T}) \cdot (\nabla \phi) \, dx - \int_{\Omega_B} f \phi \, dx = 0. \tag{9}$$

By the arbitrariness of ϕ and under suitable regularity assumptions for the temperature fields, we can apply the fundamental lemma of the calculus of variations and obtain $f = 0$ on the physical domain Ω_D and the expression of the fictitious source inside the cavity Ω_C as

$$f = \rho c \partial_t \tilde{T} - k \Delta \tilde{T}, \tag{10}$$

with $k \nabla \tilde{T} \cdot \boldsymbol{n} = 0$ and $\tilde{T} = T$ on $\partial\Omega_C$.

We can conclude that, given a solution T of the physical problem (5), a fictitious source f to be used in (6) to correctly reproduce the temperature field on the physical domain can be constructed as follows:

1. Set $f = 0$ on the physical domain Ω_D.
2. Find any extension $\tilde{T}$ to the cavity domain Ω_C of the physical temperature field T, in such a way that the boundary conditions $k \nabla \tilde{T} \cdot \boldsymbol{n} = 0$ and $\tilde{T} = T$ on $\partial\Omega_C$ are satisfied at all times.
3. Use Eq. (10) to compute the fictitious source inside the cavity Ω_C.

If boundary data require using weak solutions in Sobolev spaces rather than smooth ones, we shall interpret the foregoing identities as holding almost everywhere in the respective domains. □

Clearly, there is no unique way to obtain an extension with the sought properties. If the domain has a very simple shape we may explicitly write smooth extensions, but we propose here a strategy that allows to select a specific extension whenever Ω_C has a Lipschitz boundary. We fix a characteristic length ε (say, the diameter of Ω_C) and, for each time instant, consider the unique solution of the differential problem

$$\begin{cases} -\Delta(\tilde{T} - \varepsilon^2 \Delta \tilde{T}) = 0 & \text{on } \Omega_C, \\ \tilde{T} = T & \text{on } \partial\Omega_C, \\ \nabla \tilde{T} \cdot \boldsymbol{n} = 0 & \text{on } \partial\Omega_C. \end{cases} \tag{11}$$

Existence and uniqueness of solution to (11) can be easily proved with standard techniques in the calculus of variations. Indeed, it is enough to look for minimizers of a convex functional, equivalent to the squared H^2-norm, on the closed convex subset of $H^2(\Omega_C)$ identified by the boundary conditions [25]. We expect extensions found in this way to feature smaller gradients and be more amenable to numerical approximations. A further crucial aspect in choosing a fourth-order differential operator to determine the extension is that it allows to impose boundary conditions on both the solution and its normal derivative on all of the boundary. This would be impossible if we were to use, for example, a second-order operator such as the Laplacian.

Even though there are infinite possible choices for the temperature extension and, as a consequence, for the fictitious source f, we stress that all of them do vanish in the physical domain Ω_D, while possibly being discontinuous at the cavity boundary $\partial\Omega_C$. This represents a good feature if one wishes to use fictitious sources to determine the shape of voids within the physical domain.

3. A numerical example

We shall now illustrate the theoretical result of the previous section by means of an explicit comparison taking the filled domain $\Omega_B \subset \mathbb{R}^2$ as the rectangle of width 0.41 and height 2.2 (in arbitrary units of length) and the cavity Ω_C as the circle with radius $R = 0.1$ and centered in $O = (0.2, 0.2)$. We consider a time-dependent boundary condition that represents a thermal flash $g(\boldsymbol{x}, t) = 5 \cdot 10^7 t \exp(-10\sqrt{5t})$ on the bottom side of Ω_B and $g(\boldsymbol{x}, t) = 0$ on the rest of the boundary. Since the cavity is circular, we consider polar coordinates $(r, \theta) \in [0, R] \times [0, 2\pi)$ centered in O. We denote by $T^{\mathrm{e}}(t, \theta)$ the value of the temperature on the cavity boundary $\partial\Omega_C$ as given by the solution of the physical problem (5). To find the extension $\tilde{T}$, we consider the Fourier series expansions

$$T^{\mathrm{e}}(t, \theta) = \sum_{j=0}^{\infty} \hat{T}_j^{\mathrm{e}}(t) \exp(-j\theta \mathrm{i}) \qquad \text{and} \qquad \tilde{T}(t, r, \theta) = \sum_{j=0}^{\infty} \hat{T}_j(t, r) \exp(-j\theta \mathrm{i}). \tag{12}$$

If we now substitute $\varepsilon = R$ and the above expansion of $\tilde{T}$ in (11) and use the orthogonality of the Fourier basis, we obtain the equations

$$\hat{T}_j \frac{j^2}{r^2}\left(\frac{3R^2}{r^2} - 1\right) + \frac{\partial \hat{T}_j}{\partial r}\frac{1}{r}\left(1 - \frac{R^2}{r^2}(1 + 2j^2)\right) + \frac{\partial^2 \hat{T}_j}{\partial r^2}\left(1 + \frac{R^2}{r^2}(1 + 2j^2)\right) - \frac{2R^2}{r}\frac{\partial^3 \hat{T}_j}{\partial r^3} - R^2 \frac{\partial^4 \hat{T}_j}{\partial r^4} = 0 \tag{13}$$

for each $j \in \mathbb{N}$, with boundary conditions

$$\hat{T}_j(t, R) = \hat{T}_j^{\mathrm{e}}(t), \qquad \partial_r \hat{T}_j(t, R) = 0 = \partial_r \hat{T}_j(t, 0), \qquad \lim_{r \to 0} |\hat{T}_j(t, r)| < \infty. \tag{14}$$

By introducing the dimensionless variable $y = r/R$, we can express the general solutions of (13) as

$$\hat{T}_0(t, Ry) = c_1^0(t) + c_2^0(t)\log(y) + c_3^0(t) I_0(y) + c_4^0(t) K_0(y) \qquad \text{if } j = 0, \tag{15}$$

$$\hat{T}_j(t, Ry) = c_1^j(t) y^j + c_2^j(t) y^{-j} + c_3^j(t) I_j(y) + c_4^j(t) K_j(y) \qquad \text{if } j > 0, \tag{16}$$

where $I_n(y)$ and $K_n(y)$ are modified Bessel functions of order n [26]. The time-dependent coefficients $c_i^j(t)$ for $i = 1, \ldots, 4$ are determined by the boundary conditions (14) and lead to the solution

$$\hat{T}_0(t, r) = \hat{T}_0(t, Ry) = \hat{T}_0^{\mathrm{e}}(t) \qquad \text{if } j = 0, \tag{17}$$

$$\begin{aligned} \hat{T}_j(t, r) &= \hat{T}_j(t, Ry) \\ &= \left[\frac{(I_{j-1}(1) + I_{j+1}(1))}{2j I_{j+1}(1)} y^j - \frac{I_j(y)}{I_{j+1}(1)}\right] \hat{T}_j^{\mathrm{e}}(t) =: \alpha_j(y) \hat{T}_j^{\mathrm{e}}(t) \qquad \text{if } j > 0. \end{aligned} \tag{18}$$

From these, we can finally compute the fictitious source

$$f(t, r, \theta) = \rho c \frac{\partial}{\partial t}\tilde{T} - k\Delta\tilde{T} = \rho c \frac{\partial}{\partial t}\hat{T}_0^{\mathrm{e}}(t) + \sum_{j=0}^{\infty}\left[\rho c \alpha_j(y) \frac{\partial}{\partial t}\hat{T}_j^{\mathrm{e}}(t) + \frac{k}{R^2}\hat{T}_j^{\mathrm{e}}(t)\frac{I_j(y)}{I_{j+1}(1)}\right]\exp(-j\theta\mathrm{i}). \tag{19}$$

To verify the coherence of the solution of the heat conduction problem (5) on the domain Ω_D with the one of Problem (6) on Ω_B with the fictitious source given by (19), we implemented a finite-element discretization using the Python library FEniCS [27,28]. Since $T^{\mathrm{e}}(t, \theta)$ is known only on a discrete set of mesh points, we need to perform, at each time step, a discrete Fourier transform to obtain the coefficients in (19). Within the approximation accuracy, we find an excellent agreement between the two solutions (Fig. 1).

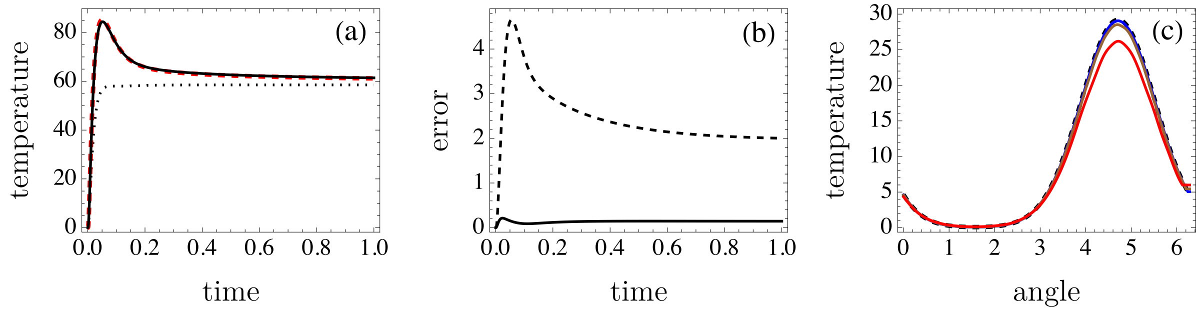

Fig. 1. The source term added on the filled domain well simulates the void. (a) The physical temperature evolution at one point on the cavity boundary (red dashed line) is well captured by the solution of the problem with a fictitious force (black solid line), whereas the heat equation on the filled domain and without source term (dotted line) gives a very different prediction. (b) The global error given by the L^2-norm of the difference, on the physical domain, between the physical temperature and the one obtained with the fictitious force (solid line) is much lower than what would be predicted (dashed curve) using a filled domain and without the fictitious source. (c) The grid refinement is crucial to obtain a good approximation of the datum at the cavity boundary. Here we show the comparison between boundary data obtained by interpolation (black dashed line) and its reconstruction with Fourier series expansions as the number of mesh nodes on the cavity varies: $40, 80, 160$ nodes (red, brown, blue line respectively). (For interpretation of the references to color in this figure legend, the reader is referred to the web version of this article.)

4. Paving the way for the inverse problem

The opportunity of substituting a void with an equivalent fictitious heat source, proven in Section 2.1, allows to reformulate the inverse problem of identifying voids from temperature measurements as an equivalent source estimation problem. Prior to the present study, this fact has been confirmed only by mere intuition and algorithmic exploration [13] which, however, made it evident that estimating the fictitious heat source turns out to be much easier than estimating the void by solving a geometric inverse problem (see e.g. [9,13] and the references therein). Indeed, the geometric inverse problem has a nonlinear formulation and requires a two-level iterative optimization algorithm, while heat source estimation is a linear problem.

Focusing on source estimation, mathematical results about inverse heat transfer problems ensure that under suitable hypotheses, e.g. if it is known that the source expression has separable variables, it is possible to uniquely reconstruct both the temperature evolution and the source term from time-dependent boundary data (see theorems 6.1, 6.2 and 6.3 in [3]). However, in our example we have chosen the extension as solution of (11) and we obtained the source (19) where variables are not separable in the way required by the cited theorems, as it may often occur. To deal with generic situations, we must therefore introduce a numerical estimator that should infer the fictitious heat sources from a restricted set of available data. More precisely, we point toward a model-based estimator, where the model is given by the Eqs. (6) through the algebraic inversion of their discretization in space and time.

Here we study the behavior of this algebraic inversion of the model with respect to the obtainable degree of knowledge about the temperature field values inside the domain. The aim is to show how the information about the void boundary is at least partially retained, as the number of temperature-measurement points decreases. Let us start by supposing to know all the temperatures $\tilde{T}$ that satisfies (6) on Ω_B, i.e. all the temperatures on the physical domain plus the fictitious temperature extension inside the void region. We consider the problem (6) discretized in space, using the Finite Element Method (FEM) with Lagrangian elements P1, and in time, with implicit Euler method, that reads, at iteration n,

$$M\frac{\tilde{T}_n-\tilde{T}_{n-1}}{dt}+K\tilde{T}_n=f_n \qquad \Rightarrow \qquad \underbrace{(I+dt\ M^{-1}K)}_{A}\tilde{T}_n=\tilde{T}_{n-1}+\underbrace{dt\ M^{-1}}_{B}f_n,$$

where M and K are the mass and stiffness matrices of the FEM discretization, dt is the time step chosen in the time-discretization and f_n is the fictitious heat source at time t_n. Therefore, we get the estimate $\hat{f}_n$ from

$$B\ \hat{f}_n=A\ \tilde{T}_n-\tilde{T}_{n-1}. \tag{20}$$

Notice that, thanks to the correspondence between the support of the fictitious heat source and the void region, solving the previous system allows to identify and localize the void, if its solution approximates the fictitious heat source with a sufficient accuracy (see Fig. 2(a–c)).

As a further step, let us now assume that, as happens in a real application, we do not have a complete knowledge of all measurements $\tilde{T}$ because, for example, not all temperatures are detectable by the physical instruments. Precisely, in Fig. 2(c) we suppose to known all the temperatures on the physical domain Ω_D, in Fig. 2(d) we suppose to known all the temperatures on the extended domain Ω_B at mesh nodes with a y coordinate $y \leq 0.32$, in Fig. 2(e) with $y \leq 0.24$ and in Fig. 2(f) with $y \leq 0.08$. Note that this method gives the projection of the void/source support on the domain region where temperatures are known. This is not surprising, anyway: when we drop the unknown temperatures from $\tilde{T}$, the right-hand-side of (20) remains sparse and localized within the region of the retained components of $\tilde{T}$, i.e. the region where the temperatures are known, thanks to the typical sparsity

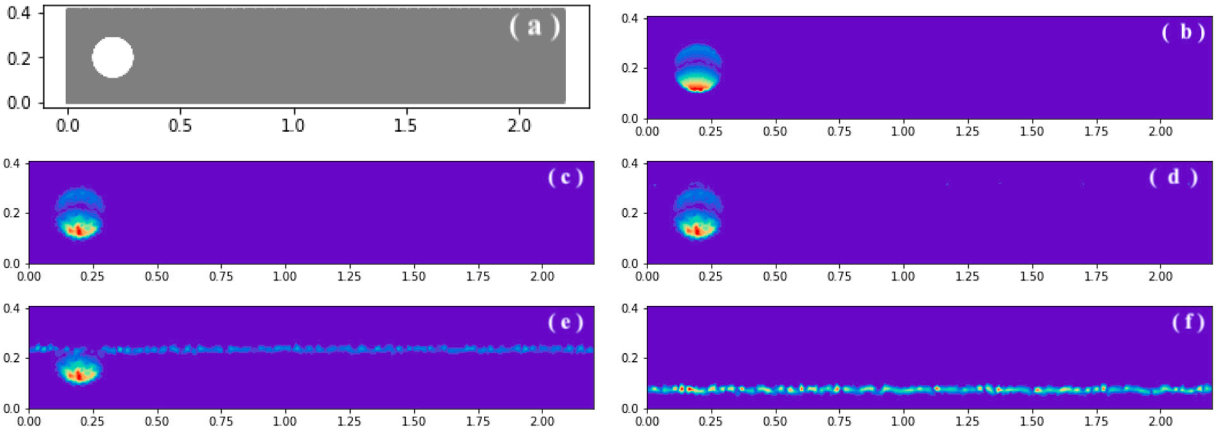

Fig. 2. The rectangular domain Ω_B : $[0.0, 2.2] \times [0.0, 0.41]$ (a), the absolute value of the fictitious source term $|f(t, r, \theta)|$ (b) and its algebraic reconstruction with the sparsity constraint in different conditions as a rainbow color map (max value = red, min value = blue): when all temperatures on Ω_D are known (c), when all temperatures on Ω_B with $y \leq 0.32$ are known (d), when all temperatures on Ω_B with $y \leq 0.24$ are known (e), when all temperatures on Ω_B with $y \leq 0.08$ are known (f). (For interpretation of the references to color in this figure legend, the reader is referred to the web version of this article.)

pattern of finite element matrices and for the same reasons it holds also for the estimated heat source $\hat{f}_n$. Finally, to enforce $\hat{f}_n$ to have a compact support, we have imposed the sparsity constraint [29] to solve the under-determined system resulting from pre-multiplying both terms of Eq. (20) by the inverse of the matrix A and dropping the equations corresponding to the unknown temperatures:

$$\hat{A}^{-1} \cdot \hat{B}\hat{f}_v = \hat{T}_n - \hat{A}^{-1}\tilde{T}_{n-1}. \tag{21}$$

The best results have been obtained with a variant [30] of the well-known Lawson–Hanson algorithm, for its better robustness against not-too-well conditioned matrices and not-too-sparse problems, compared to greedy algorithms for sparse recovery, like the Orthogonal Matching Pursuit [29]. However, the reformulation (21) with the sparsity constraint was not able to significantly reconstruct the void/source support outside the domain region where temperatures are known, thus again confirming the need to reconstruct the full field of temperatures, for instance with a Kalman Filter, repeatedly mentioned during the bibliography survey made in the Introduction.

5. Conclusions

In this work, we have shown how to represent material changes, in the context of diffusion or wave propagation problems, by means of fictitious forcing terms, with the goal of simplifying the formulation of inverse problems aimed at reconstructing the region of varying parameters from a limited set of boundary measurements. Analyzing a paradigmatic heat conduction problem on a domain with a cavity, we have proven that the presence of the void can be replaced by a fictitious heat source with support contained inside the cavity.

This fact has been illustrated in a situation where the source term can be analytically recovered from the values of the temperature and heat flux at the boundary of the cavity. Thanks to this result, the nonlinear geometric inverse problem of void identification is simplified into a linear and more manageable one, that involves the identification of forcing terms given the knowledge of boundary data.

We then studied the algebraic reconstruction problem. Here, the main observation that a pure algebraic reconstruction gives the projection of void/source support on the domain region where temperatures are known is key to realize that the inverse problem solution method should, in some way, estimate the full field of temperatures, to be able to locate accurately the support of the fictitious heat source, and thus the void geometry. Note that the algebraic reconstruction may be used also as a prior in Bayesian learning methods (e.g. Kalman Filters) to locate the fictitious forcing term.

Finally, we stress that the proposed scheme can be adapted to a large number of initial- and boundary-value problems to help simplifying the treatment of inverse problems in several applied contexts.

Declaration of competing interest

The authors declare that they have no known competing financial interests or personal relationships that could have appeared to influence the work reported in this paper.

Data availability

Data will be made available on request.

Acknowledgments

L.R. acknowledges the financial support of the Italian Government through the “Programma Operativo Nazionale Ricerca e Innovazione” 2014–2020 (CCI 2014IT16M2OP005), fellowship number DOT1319984-2. The work of L.R. and F.M. is partially supported by the “Gruppo Nazionale per il Calcolo Scientifico” (GNCS - INdAM), Italy, and the work of G.G.G. is partially supported by the “Gruppo Nazionale per la Fisica Matematica” (GNFM - INdAM), Italy.

References

[1] Jackson JD. Classical electrodynamics. John Wiley & Sons; 2021.
[2] Kim S, Karrila SJ. Microhydrodynamics: Principles and selected applications. Courier Corporation; 2013.
[3] Lesnic D. Inverse problems with applications in science and engineering. Chapman and Hall/CRC; 2021, http://dx.doi.org/10.1201/9780429400629.
[4] Maldague X, Marinetti S. Pulse phase infrared thermography. J Appl Phys 1996;79(5):2694–8. http://dx.doi.org/10.1063/1.362662.
[5] Kassab AJ, Pollard JE. Cubic spline anchored grid pattern algorithm for high-resolution detection of subsurface cavities by the IR-CAT method. Numer Heat Transfer B 1994;26(1):63–77. http://dx.doi.org/10.1080/10407799408914917.
[6] Divo E, Kassab AJ, Rodriguez F. An efficient singular superposition technique for cavity detection and shape optimization. Numer Heat Transfer B 2004;46(1):1–30. http://dx.doi.org/10.1080/10407790490436624.
[7] Kirsch A. An introduction to the mathematical theory of inverse problems. Springer; 2021, http://dx.doi.org/10.1007/978-3-030-63343-1.
[8] Bryan K, Caudill L. Reconstruction of an unknown boundary portion from Cauchy data in n dimensions. Inverse Problems 2005;21:239–55. http://dx.doi.org/10.1088/0266-5611/21/1/015.
[9] Marcuzzi F, Marinetti S. Efficient reconstruction of corrosion profiles by infrared thermography. J Phys Conf Ser 2008;124:012033. http://dx.doi.org/10.1088/1742-6596/124/1/012033.
[10] Kazemzadeh-Parsi MJ, Daneshmand F. Cavity-shape identification with convective boundary conditions using non-boundary-fitted meshes. Numer Heat Transfer B 2010;57(4):283–305. http://dx.doi.org/10.1080/10407790.2010.481496.
[11] Sidi HO, Huntul M, Sidi MO, Emadifar H. Identifying an unknown coefficient in the fractional parabolic differential equation. Results Appl Math 2023;19:100386. http://dx.doi.org/10.1016/j.rinam.2023.100386.
[12] Pratama DA, Bakar MA, Ibrahim NF, Idris R, Mohamed N. Physical restriction neural networks with restarting strategy for solving mathematical model of thermal heat equation for early diagnose breast cancer. Results Appl Math 2023;19:100384. http://dx.doi.org/10.1016/j.rinam.2023.100384.
[13] Dessole M, Marcuzzi F. Accurate detection of hidden material changes as fictitious heat sources from thermographic data. Numer Heat Transfer B 2023. http://dx.doi.org/10.1080/10407790.2023.2220905.
[14] Ihlenburg F. Finite element analysis of acoustic scattering. Applied mathematical sciences, Springer New York; 2006.
[15] Symes WW. Wavefield reconstruction inversion: an example. Inverse Problems 2020;36(10):105010. http://dx.doi.org/10.1088/1361-6420/abaf66.
[16] Winebrenner DP, Sylvester J. Linear and nonlinear inverse scattering. SIAM J Appl Math 1998;59(2):669–99. http://dx.doi.org/10.1137/S0036139997319773.
[17] Claerbout J. Basic earth imaging. 2010, URL https://sepwww.stanford.edu/sep/prof/index.html.
[18] Bolzon G, Fedele R, Maier G. Parameter identification by Kalman filter of a cohesive crack model. Comput Methods Appl Mech Engrg 2002;191:2847–71. http://dx.doi.org/10.1016/S0045-7825(02)00223-2.
[19] Corigliano A, Mariani S. Parameter identification in explicit structural dynamics: Performance of the extended Kalman filter. Comput Methods Appl Mech Eng 2004;193. http://dx.doi.org/10.1016/j.cma.2004.02.003.
[20] Marcuzzi F. Space and time localization for the estimation of distributed parameters in a finite element model. Comput Methods Appl Mech Engrg 2009;198(37–40):3020–5. http://dx.doi.org/10.1016/j.cma.2009.05.007.
[21] Lourens E-M, Reynders E, De Roeck G, Degrande G, Lombaert G. An augmented Kalman filter for force identification in structural dynamics. Mech Syst Signal Process 2012;27:446â–60. http://dx.doi.org/10.1016/j.ymssp.2011.09.025.
[22] Arridge S. Optical tomography in medical imaging. Inverse Problems 1999;15(2):R41. http://dx.doi.org/10.1088/0266-5611/15/2/022.
[23] Alacam B, Yazici B, Intes X, Chance B. Extended Kalman filtering for the modeling and analysis of ICG pharmacokinetics in cancerous tumors using NIR optical methods. IEEE Trans Biomed Eng 2006;53(10):1861–71. http://dx.doi.org/10.1109/TBME.2006.881796.
[24] Baez GR, Pomarico JA, Elicabe GE. An improved extended Kalman filter for diffuse optical tomography. Biomed Phys Eng Express 2017;3(1):015013. http://dx.doi.org/10.1088/2057-1976/3/1/015013.
[25] Brezis H. Functional analysis, sobolev spaces and partial differential equations. Springer; 2011.
[26] Lebedev NN. Special functions and their applications. Prentice–Hall; 1965.
[27] Logg A, Mardal K, Wells GN, et al. Automated solution of differential equations by the finite element method. Springer; 2012, http://dx.doi.org/10.1007/978-3-642-23099-8.
[28] Alnaes MS, Blechta J, Hake J, Johansson A, Kehlet B, Logg A, et al. The FEniCS project version 1.5. Arch Numer Softw 2015;3. http://dx.doi.org/10.11588/ans.2015.100.20553.
[29] Elad M. Sparse and redundant representations: From theory to applications in signal and image processing. Springer Publishing Company, Incorporated; 2010.
[30] Dessole M, Dell'Orto M, Marcuzzi F. The Lawson–Hanson algorithm with deviation maximization: Finite convergence and sparse recovery. Numer Linear Algebra Appl 2023;e2490. http://dx.doi.org/10.1002/nla.2490.